SOCIETY FOR EXPERIMENTAL BIOLOGY

Journal of Experimental Botany
Advance Access Publication 17 September, 2022
This paper is available online free of all access charges (see https://academic.oup.com/jxb/pages/openaccess for further details)

Journal of Experimental Botany

RESEARCH PAPER

Temperature-induced changes in Arabidopsis Rubisco activity and isoform expression

Amanda P. Cavanagh[1,2,3,*], Rebecca Slattery[2] and David S. Kubien[1]

[1] Department of Biology, University of New Brunswick, Fredericton, NB, E3B 5A3, Canada
[2] Carl R. Woese Institute for Genomic Biology, University of Illinois at Urbana-Champaign, Urbana, IL 61801, USA
[3] School of Life Sciences, University of Essex, Colchester CO4 3SQ, UK

* Correspondence: a.cavanagh@essex.ac.uk

Received 30 April 2022; Editorial decision 26 August 2022; Accepted 16 September 2022

Editor: Robert Sharwood, Western Sydney University, Australia

Abstract

In many plant species, expression of the nuclear encoded Rubisco small subunit (SSu) varies with environmental changes, but the functional role of any changes in expression remains unclear. In this study, we investigated the impact of differential expression of Rubisco SSu isoforms on carbon assimilation in Arabidopsis. Using plants grown at contrasting temperatures (10 °C and 30 °C), we confirm the previously reported temperature response of the four *RbcS* genes and extend this to protein expression, finding that warm-grown plants produce Rubisco containing ~65% SSu-B and cold-grown plants produce Rubisco with ~65% SSu-A as a proportion of the total pool of subunits. We find that these changes in isoform concentration are associated with kinetic changes to Rubisco *in vitro*: warm-grown plants produce a Rubisco having greater CO_2 affinity (i.e. higher $S_{C/O}$ and lower K_C) but lower k_{catCO_2} at warm measurement temperatures. Although warm-grown plants produce 38% less Rubisco than cold-grown plants on a leaf area basis, warm-grown plants can maintain similar rates of photosynthesis to cold-grown plants at ambient CO_2 and 30 °C, indicating that the carboxylation capacity of warm-grown Rubisco is enhanced at warmer measurement temperatures, and is able to compensate for the lower Rubisco content in warm-grown plants. This association between SSu isoform expression and maintenance of Rubisco activity at high temperature suggests that SSu isoform expression could impact the temperature response of C_3 photosynthesis.

Keywords: Arabidopsis, carboxylation, oxygenation, phenotypic plasticity, photosynthesis, Rubisco.

Introduction

Ribulose-1,5-bisphosphate carboxylase/oxygenase (Rubisco) catalyses the competing reactions of photosynthetic carboxylation of ribulose-1,5-bisphosphate (RuBP) and photorespiratory RuBP oxygenation. Since it is a dual-substrate enzyme, a defining kinetic feature is the enzyme's CO_2/O_2 specificity factor ($S_{C/O}$), which is the ratio of the catalytic efficiencies of its carboxylation reaction (k_{catCO_2}/K_C) and oxygenation reaction (k_{catO_2}/K_O), where k_{cat} is the enzyme's turnover rate and K_C and K_O are the apparent Michaelis–Menten constant for each substrate. Rubisco is approximately 2000 times more

Abbreviations: A_N, net CO_2 assimilation; C_a, CO_2 concentration in air; C_i, intercellular airspace CO_2 concentration; C_c, chloroplastic CO_2 concentration; E_a, activation energy; g_m, mesophyll conductance to CO_2; g_s, stomatal conductance to CO_2; J_{max}, maximal rate of electron transport; K_C, Michaelis–Menten constant of Rubisco for CO_2; $K_{C21\%O_2}$, Michaelis–Menten constant of Rubisco for CO_2 in the presence of 21% O_2; k_{catCO_2}, catalytic turnover rate of Rubisco carboxylation; K_O, Michaelis–Menten constant of Rubisco for O_2; LSu, Rubisco large subunit; *rbcL*, gene encoding Rubisco large subunit; *RbcS*, gene encoding Rubisco small subunit; RuBP, ribulose-1,5-bisphosphate; $S_{C/O}$, Rubisco substrate specificity; SSu, Rubisco small subunit; Γ^*, CO_2 compensation point; V_c, Rubisco carboxylation rate; V_{cmax}, maximal rate of carboxylation.

specific for CO_2 than O_2, but because the latter is some 500 times more abundant in today's atmosphere, RuBP oxygenation is a significant limitation to carbon gain, and plays an important role in the photosynthetic temperature response (Sage and Kubien, 2007; Moore *et al*., 2021).

As temperatures rise, the rate of both Rubisco carboxylation and oxygenation increase, as increased temperatures lower the activation barrier for the addition of both substrates (Sage, 2002; Galmés *et al*., 2015). However, the carboxylation:oxygenation ratio decreases as temperatures rise, both because the ratio of $[CO_2]$:$[O_2]$ in solution and Rubisco $S_{C/O}$ decline. Consequently, photorespiration increases with rising temperature, limiting potential growth and productivity (Walker *et al*., 2016), making photorespiration an important bioengineering target for crop improvement and resilience (South *et al*., 2019; Roell *et al*., 2021; Cavanagh *et al*., 2022). The increased photorespiratory pressure of hot, dry, arid environments has driven the evolution of carbon concentrating mechanisms, including C_4 and C_2 photosynthesis (Lundgren and Christin, 2016; Sage *et al*., 2018). Within C_3 plants, there is evidence that warm growth temperatures can also alter Rubisco $S_{C/O}$ or thermotolerance, improving Rubisco performance and carbon assimilation at warm growth temperatures (Yamori *et al*., 2006; Cavanagh and Kubien, 2014). Yamori *et al*. (2006) found that Rubisco from cold-grown (15/10 °C) *Spinacia oleracea* (spinach) is 5% more specific for CO_2 than O_2 at 10 °C than Rubisco from warm-grown (30/25 °C) plants, but when measured at 35 °C, the warm-grown Rubisco is 11% more specific. Theoretically, the growth temperature-mediated changes in spinach Rubisco $S_{C/O}$ may convey a carbon-gain advantage during acclimation (Cavanagh and Kubien 2014). The mechanism behind these kinetic changes is not apparent, but likely involve some structural changes to the enzyme.

In land plants and green algae, Rubisco is a hexadecameric complex of eight large and eight small polypeptide subunits (referred to as an L8S8 enzyme form). The Rubisco catalytic site is located at the interface of two 55 kDa large subunits (LSu), which are encoded by the *rbcL* gene in the chloroplast genome. The 15 kDa small subunits (SSu) are produced in the cytosol by nuclear-encoded *RbcS* genes and imported to the chloroplast. Though not directly involved in catalysis, the SSus are required for maximum Rubisco activity (Andrews, 1988). Further, Rubisco containing SSu mutations, or hybrid Rubiscos with native LSus and foreign SSus, often have altered holoenzyme stability and kinetic properties (Spreitzer *et al*., 2005; Ishikawa *et al*., 2011; Sharwood *et al*., 2016; Martin-Avila *et al*., 2020).

The nuclear encoded *RbcS* genes have more sequence diversity than the chloroplastic *rbcL*, and in many species are present in multigene families ranging from two copies in *Chlamydomonas* to 22 copies in several *Flaveria* species (Spreitzer, 2003; Kapralov *et al*., 2010). Within the multigene family, differential *RbcS* gene expression has been reported in response to environmental and development cues in a range of species (Wanner and Gruissem, 1991; Dedonder *et al*., 1993; Meier *et al*., 1995; Cheng *et al*., 1998; Eilenberg *et al*., 1998; Yoon *et al*., 2001; Suzuki *et al*., 2009). Arabidopsis has four *RbcS* genes that show differential expression in response to environmental parameters such as light, CO_2, and temperature (Dedonder *et al*., 1993; Cheng *et al*., 1998; Yoon *et al*., 2001; Sawchuk *et al*., 2008). However, the impact of these gene-expression changes on Rubisco structure and performance remains unclear.

Unlike the widespread interspecific variation in *RbcS* sequence and copy number, the SSu amino acid sequences within a single species are fairly well conserved. For example, in *Solanum tuberosum* (potato) SSu isoforms have 93% sequence identity. However, Martin-Avila *et al*. (2020) engineered tobacco plants to express L8S8 Rubisco containing both the potato LSu and a single potato SSu isoform, and found that Rubisco containing only the SSu-3 isoform had a 9% increase in k_{catCO2} coupled with impaired protein synthesis, which translated into changes in growth and photosynthetic carbon gain. Thus, it is clear that even small differences in amino acid sequence can impart physiologically relevant changes in Rubisco's kinetic phenotype. By contrast, the four Arabidopsis SSu peptides share a 97% sequence similarity, and *RbcS* mutant lines expressing different SSu complements do not show altered photosynthetic phenotypes in today's atmosphere (Izumi *et al*., 2012; Khumsupan *et al*., 2020), nor are the kinetic properties of these Rubiscos different at 25 °C (Atkinson *et al*., 2017). However, the potential kinetic contribution of alternative SSu isoforms under variable environmental conditions has not been fully explored (Cavanagh and Kubien, 2014; Cavanagh, 2020).

In Arabidopsis, gene-specific expression within the *RbcS* family varies with both temperature and CO_2 conditions; growth at low temperatures or high CO_2 increases *RbcS1A* expression, while growth at high temperatures or ambient CO_2 increases *RbcS3B* expression (Cheng *et al*., 1998; Yoon *et al*., 2001), but changes in *RbcS* gene expression have not been correlated with changes in Rubisco performance. In this work, we aim to determine: (i) if the differences in *RbcS* expression correlate with Rubisco protein expression under different growth temperature regimes; (ii) whether this difference corresponds with changes in Rubisco kinetics *in vitro*; and finally (iii) whether these *in vitro* differences impact the photosynthetic phenotype *in vivo*.

Materials and methods

Plant growth and sampling

Arabidopsis (Col-0) seeds were stratified for 3 d at 4 °C on Promix (Plant Products, Brampton, Canada), transferred to a growth chamber (E-15 Conviron, Winnipeg, Manitoba, Canada) and grown under photoperiod conditions of 10 h light/14 h dark, 20/18 °C, 300 μmol m^{-2} s^{-1} photosynthetic photon flux density, under ambient (400–450 μmol mol^{-1}) and elevated (1000 μmol mol^{-1}) CO_2 levels. After 1 week, plants were transferred to either a warm (30/27 °C), a cold (10/8 °C), or a moderate (20/18 °C) growth temperature treatment. Temperature and CO_2 treatments were applied as a factorial design over two growth chambers, swapping chambers account for any chamber effects (Supplementary Fig. S1). Leaf temperatures (measured with thermocouples) during the 'day' were 8.8, 19.2, and 27.4 °C at 10, 20, and 30 °C air temperatures, respectively. Plants were watered to excess every 2 d (at 30 °C), and every 4 d (10 °C and 20 °C) with a modified Hoagland's nutrient solution. To normalize nitrogen application to a rate of 160 mmol N week^{-1}, 30 °C plants with a solution containing 8 mM total N, and 20 °C- and 10 °C-grown plants were watered with a 16 mM total N solution. Leaf tissue for RNA extraction and biochemical analyses was sampled from the youngest fully expanded leaf of the fourth whorl of 5- to 6-week-old plants (growth stage 3.70–3.90). Leaf discs were obtained 6–7 h after simulated dawn, flash frozen in liquid nitrogen, and stored at −80 °C until extraction.

Total plant RNA extraction and cDNA synthesis

Total RNA was extracted from flash-frozen leaf material using the RNeasy Plant RNA extraction kit (Qiagen, Hilden, Germany) according to the manufacturer's instructions. Concentration and relative purity were measured using a spectrophotometer (NanoVue, GE Healthcare Life Sciences), and RNA integrity was confirmed visually on an agarose gel stained with SYBRSafe (Thermo Fisher Scientific). One microgram of RNA was reverse transcribed into cDNA using the QuantiTect Reverse Transcription Kit (Qiagen). Gene expression was measured via quantitative PCR in 20 µl reaction volumes containing 10 µl KAPA SYBR FAST qPCR Master Mix (2X) (KAPA Biosystems, Woburn, MA, USA), 200 nM of gene-specific forward and reverse primers, and 1 µl of cDNA. Real time quantification of amplicons was performed using a Rotor-Gene 6000 thermal cycler (Corbett Life Sciences, Sydney, NSW, Australia), using the following standard thermal profile for all reactions: 95 °C for 2 min, followed by 40 cycles of 95 °C for 3 s, 58 °C for 20 s, and 72 °C for 2 s. Primers for *rbcL* were 5′-GTGTTGGGTTCAAAGCTGGT-3′ and 5′-CATCGGTCCACACAGTTGTC-3′ (Supplementary Table S1). Primers flanked regions in the 3′ UTR of each *RbcS* gene, using a common reverse primer for both *RbcS1A* and *RbcS3B* genes. Product specificity was confirmed visually by band presence/absence following agarose electrophoresis, and via dissociation curves with single peaks obtained for each reaction product.

To extrapolate absolute expression of mRNA copy numbers from the RT-qPCR assay, gene-specific standard curves were prepared in triplicate from known copy numbers of plasmids containing the target sequence of each primer set. All plasmid dilutions used for the standard curves amplified consistently, indicating a linear amplification range of at least six orders of magnitude, from 10^2 to 10^8 copies µl^{-1}. Expression was normalized to a reference gene (*AT1G13320*), which is consistently expressed across changes in growth temperature in Arabidopsis (Czechowski *et al.*, 2005). Controls containing no template cDNA (NTC) and total RNA (no-RT) were included in every run, and they were not amplified below PCR cycles nor did they cross the quantification cycle threshold (C_q) for samples included in the analysis.

Rubisco immunoblotting

To examine changes in SSu composition, a quantitative immunoblotting procedure modified from Yamori and von Caemmerer (2011) was used, using a dilution of chromatographically purified spinach Rubisco as a standard. Three micrograms of total Arabidopsis soluble protein and 0.25–2 µg of spinach Rubisco standard in Laemmli buffer (2% SDS, 10% glycerol, 60 mM Tris-Cl pH 6.8) were denatured at 100 °C for 3 min and separated with SDS-PAGE on a 22.4 cm 4–20% acrylamide gel. Proteins were visualized with Coomassie Brilliant Blue (R-250), or transferred to polyvinylidene difluoride membranes pre-wetted in methanol and equilibrated in transfer buffer (2.5 mM Tris, 19.2 mM glycine, 20% methanol, pH 8.6) for 60 min at 100 V. Immediately after transfer, membranes were blocked with 3% non-fat milk (Carnation) in 20 mM Tris, 150 mM NaCl, and 0.1% (v/v) Tween-20 (TBST) for 1 h at room temperature with agitation, or 4 °C overnight. The blot was probed with a polyclonal primary anti-SSu rabbit antibody (Agrisera AS07259, Vännäs, Sweden) diluted 1:5000 in 1% milk in TBST, and an alkaline phosphatase-conjugated goat-anti-rabbit secondary antibody was used (Sigma-Aldrich A3687, St Louis, MO, USA) to develop blots using an alkaline phosphatase Immun-Blot kit (Bio-Rad Laboratories, Mississauga ON, Canada). Protein levels on immunoblots were quantified via densiometry (Quantity One Software, Bio-Rad).

Rubisco extraction and quantification

Rubisco was prepared from frozen ground leaf tissue (1.1 cm^2 disks) in a Tenbroek glass-in-glass homogenizer containing 3 ml of ice-cold extraction buffer (100 mM HEPES pH 7.6, 2 mM Na-EDTA, 5 mM $MgCl_2$, 5 mM dithiothreitol (DTT), 10 mg ml^{-1} polyvinyl polypyrrolidone, 2% (v/v) Tween-80, 2 mM NaH_2PO_4, 12 mM amino-*n*-caproic acid, and 2 mM benzamidine) and 50 µl Protease Inhibitor Cocktail (P9599, Sigma). The chlorophyll content of the leaf homogenate was determined spectrophotometrically after extraction in 80% buffered acetone (Porra *et al.*, 1989). This homogenate was centrifuged at 16 000 *g* at 4 °C for 60 s, and total soluble protein (Bradford, 1976) and k_{catCO2} measured from this freshly extracted supernatant. For Michaelis–Menten constants and $S_{C/O}$ measurements, the supernatant was desalted (Econo-Pac 10DG desalting column, Bio-Rad) and further concentrated using a spin column as described in Boyd *et al.* (2019) (Amicon 50K spin filters, Millipore, Billerica, MA, USA). Fresh and concentrated aliquots were incubated with 20 mM $MgCl_2$ and 10 mM $NaHCO_3$ at 30 °C for 20 min to fully carbamylate Rubisco. Rubisco catalytic sites in the carbamylated extract were determined using a [^{14}C]carboxy-arabinitol bisphosphate binding assay, with a specific activity of 3.1 kBq nmol^{-1} Rubisco, assuming eight binding sites per Rubisco (Kubien *et al.*, 2011). Rubisco k_{catCO2}, K_C, K_O, and $S_{C/O}$ were determined via radiolabel techniques exactly as described in Boyd *et al.* (2019).

Gas exchange measurements

The CO_2 response of net CO_2 assimilation (e.g. A_N–C_i curves) was measured using an open gas exchange system (Li-6400, LI-COR Inc., Lincoln, NE, USA). To minimize the impact of developmental stage on measurements, plants were sampled during vegetative growth (i.e. before flower formation; Flexas *et al.*, 2007). Gas exchange was measured in five plants from each growth temperature at 10 °C and 30 °C. Measurements at 10 °C were obtained in a temperature-controlled growth chamber (Conviron PGC-20, Controlled Environments Ltd). The leaf cuvette was set at a reference CO_2 (C_a) of 400 µmol mol^{-1} and saturating light (500 or 750 µmol m^{-2} s^{-1} at 10 °C and 30 °C, respectively) to reach steady state and then C_a was decreased in a stepwise fashion from 400, 200, 150, 100, 75, 50, 300, 400, 400, 500, 750, 1200 (both), 1800 (30 °C only) µmol mol^{-1} CO_2, and measurements made as soon as stability was achieved at each CO_2 level, typically within 1–3 min. Respiration (R_d) was measured following a dark-acclimation period of 10 min at 400 µmol mol^{-1} CO_2.

Estimates of mesophyll conductance (g_m), V_{cmax}, and J_{max} were obtained following the curve-fitting method of Ethier and Livingston (2004) using *in vitro* Rubisco parameter values and temperature responses of the Michaelis–Menten constant for CO_2 (K_C) and oxygen (K_O) and the CO_2 compensation point in the absence of day respiration (Γ^*) calculated from the Rubisco specificity factor ($S_{C/O}$) from warm- and cold-grown Arabidopsis. The transition point between the Rubisco and RuBP regeneration-limiting portions of the curve was determined as the C_i that minimized the difference between g_m estimates from both processes (Ethier *et al.*, 2006).

At low CO_2 concentrations the photosynthetic rate of a C_3 plant is determined by the capacity of Rubisco carboxylation, as the substrate concentration is generally below the Michaelis–Menten constant for the enzyme. To asses Rubisco carboxylation *in vivo*, the initial slopes of A_N–C_C curves from warm- and cold-grown plants measured at 10 °C and 30 °C were compared to assess Rubisco carboxylation activity *in vivo*. An *in vivo* estimate for the Rubisco Michaelis–Menten constant for CO_2 in the presence of oxygen ($K_{C21\%O2}$) was then determined by regressing individual *A*–chloroplastic CO_2 concentration (C_c) curves against a Michaelis–Menten equation of the form:

$$\frac{A}{[\text{Rubisco}]} = \frac{(C_c - \Gamma*)\, k_{\text{catCO}_2}}{C_c + K_{C21\%O_2}} \quad (1)$$

where $K_{C21\%O2}$=$K_C(1+O/K_O)$, Γ* is the compensation point, and [Rubisco] is the Rubisco site concentration.

Statistics and modeling

The temperature response of Rubisco parameters was determined by calculating in Sigmaplot (Systat Software) the activation energy from an Arrhenius relationship of the form:

$$\text{Parameter}\,(T) = \text{Parameter}\,(25\ ^\circ\text{C}) \times \exp\left[(T-25)\,E_a/298R\,(273+T)\right] \quad (2)$$

where *R* is the universal gas constant (8.314 J K^{-1} mol^{-1}), E_a is the activation energy (kJ mol^{-1}) and *T* is the assay temperature (°C). Differences in gene expression, protein expression and Rubisco content, and the activation energy and value at 25 °C for each Rubisco parameter were compared using ANOVA and post-hoc Tukey's test, considering differences to be significant at P<0.05. A two-way ANOVA (with growth and measurement temperature as main effects) was used to compare *in vivo* photosynthetic parameters, and $K_{C21\%O2}$. All statistical analysis was performed in R (R Core Team, 2020).

The CO_2 response of Rubisco carboxylation (V_C) was modelled according to the equation:

$$V_c = (V_{\text{cmax}} \times C)\,/\,(C + K_{c21\%O2}) \quad (3)$$

using k_{catCO2} as an estimate for V_{cmax}, and calculating $K_{C21\%O2}$ from the *in vitro* determined values of K_C and K_O reported in Table 2.

Results

Growth temperature alters Rubisco subunit gene and protein expression

Growth temperature alters the expression of both *rbcL* and *RbcS* transcripts (Fig. 1). Warm-grown plants produced 38% less Rubisco (measured on a leaf area basis) than plants grown at 10 °C (Table 1, P<0.05). This decrease in Rubisco content was coupled with a 56% reduction in *rbcL* transcript expression (Fig. 1B, P<0.05), and was not associated with proteolytic degradation visualized as banding on an immunoblot (Fig. 2B). The mRNA levels of *RbcS1A* and *RbcS3B*, and the ratio between them, varied with changes in growth temperature (*RbcS1A*: P=0.028; *RbcS3B*: P=0.0001 Fig. 1), but not CO_2 (*RbcS1A*: P=0.5014; *RbcS3B*: P=0.732; Supplementary Fig. S1). Transcript levels of the *RbcS1A* gene declined as growth temperature increased (Fig. 1A), while those of *RbcS3B* mRNA were higher at 30 °C versus 10 °C (Fig. 1A). As a result, at low growth temperatures *RbcS1A* dominated *RbcS* gene expression, but its mRNA levels declined by 46% when grown at 20 °C and 67% at 30 °C (Fig. 1A). By contrast, mRNA levels of *RbcS3B* were 119% higher at 30 °C than at 10 °C (Fig. 1A). At 20 °C, levels of *RbcS3B* and *RbcS1A* did not differ from expression levels in cold-grown plants at 400 or 1000 μmol mol^{-1} CO_2, but were 62% lower or 63% greater than expression levels of the respective genes at 30 °C (Fig. 1A; Supplementary Fig. S1). Growth temperature had no effect on the expression of *RbcS*1B and *RbcS*2B (Supplementary Fig. S2), and the expression of these two genes was significantly lower than that of *RbcS1A* and *RbcS3B*.

Two mature SSu proteins with different molecular mass (predicted to be 14.7 kDa and 14.8 kDa) were separate by SDS-PAGE (Fig. 2B). This separation was similar to previous reports of Arabidopsis SSu protein migration (Getzoff *et al*., 1998; Izumi *et al*., 2012). Following the nomenclature of Izumi *et al*. (2012) the larger protein is denoted as SSu-B (where the *RbcS3B* gene product is the predominant component, and has the N-terminal sequence XKVWPP; Izumi *et al*., 2012) and the smaller protein as SSu-A (which has the N-terminal sequence XQVWPP; Izumi *et al*., 2012). In cold-grown plants, SSu-A represents 62% of total SSu protein, but only 22% of total SSu protein in warm-grown plants (Fig. 2A, P<0.05). By contrast, SSu-B represents 38% and 78% of total SSu protein from 10 °C- and 30 °C-grown plants, respectively (Fig. 2A, P<0.05).

Plants from contrasting growth temperatures have kinetically distinct Rubiscos

Rubisco from plants grown at 20 °C represent an approximately intermediate phenotype in all kinetic parameters assayed (Table 2). Measured at 25 °C, Rubisco's turnover rate (k_{catCO2}) was 3.31 s^{-1} and 2.78 s^{-1} from plants grown at 10 °C and 30 °C, respectively (P<0.05). The activation energy (E_a) of k_{catCO2} did not vary with growth temperature (Table 2), but the parameter was greater than warm-grown Rubisco at measurement temperatures above 25 °C (Fig. 3A).

At 25 °C, the CO_2/O_2 specificity ($S_{C/O}$) of cold-grown Rubisco was 75.1 M M^{-1}, while in warm-grown Rubisco it was 78.0 M M^{-1} (P<0.05). The $S_{C/O}$ of cold-grown Rubisco declined more rapidly with temperature than warm-grown Rubisco, with an apparent E_a of −23.7 kJ mol^{-1} reported for Rubisco from 10 °C plants and −19.9 kJ mol^{-1} for 30 °C plants (Table 2; P<0.05). At all measurement temperatures above 20 °C, $S_{C/O}$ was greater in warm- versus cold-grown Rubisco (Fig. 3B; Supplementary Fig. S3).

At 25 °C, the Michaelis–Menten constant for CO_2 (K_C) was 11.6 μM and did not vary with growth temperature (Table 2). The activation energy (E_a) of cold-grown Rubisco K_C was 54.8 kJ mol^{-1}, while warm-grown Rubisco K_C had an E_a of 40.5 kJ mol^{-1} (Table 2, P<0.05). As a result of this change

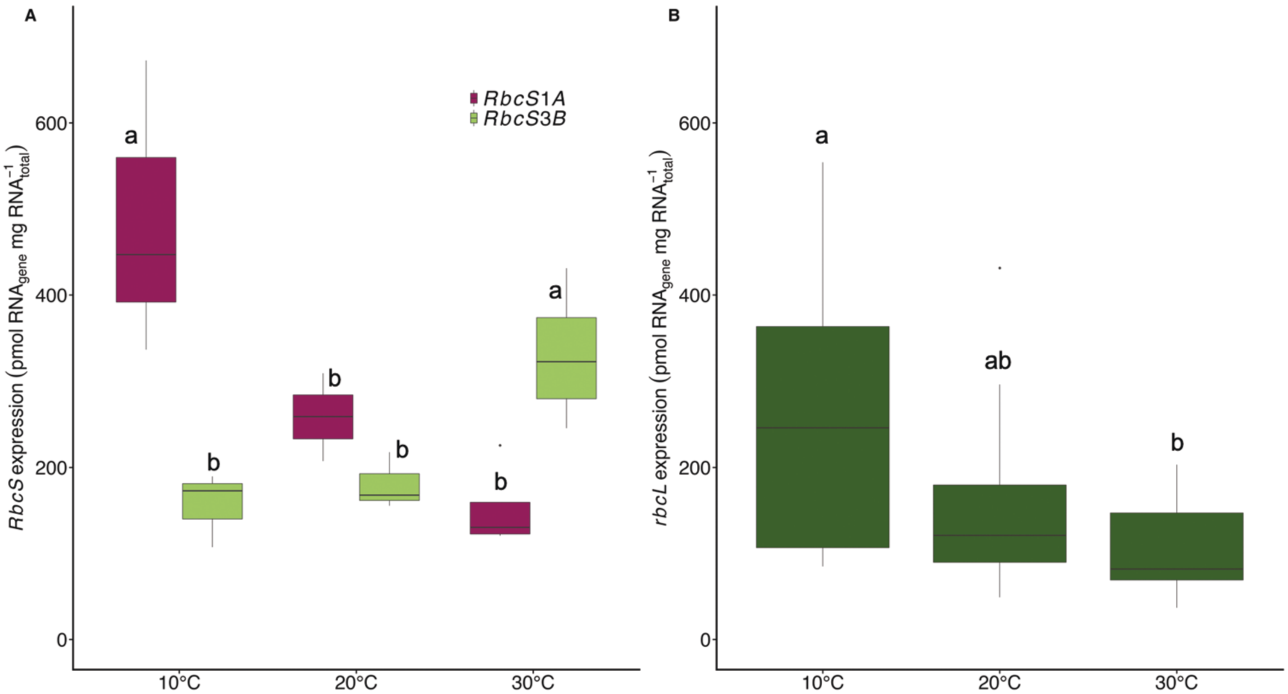

Fig. 1. Expression of Rubisco-encoding genes at ambient CO_2 conditions. Response of the two dominant members of the *RbcS* gene family (A) and *rbcL* gene expression (B) to changes in growth temperature. Gene specific expression is reported as the fraction of total RNA concentration. n=6–7. Maximum and minimum values are depicted by the bars, the box signifies the upper and lower quartiles, and the median is represented by a short black line within each box. Different letters represent significant differences in the mean of each treatment at P<0.05 (two-way ANOVA and post-hoc Tukey's HSD test). Responses of all *RbcS* genes can be found in Supplementary Fig. S2.

Table 1. Physiological parameters from plants grown at three temperatures.

	Growth temperature		
Parameter	**10 °C**	**20 °C**	**30 °C**
Rubisco content (μmol_{sites} m^{-2})	14.4 (0.83)^a	10.4 (0.32)^b	8.9 (0.61)^c
Total soluble protein (g m^{-2})	4.88 (0.9)^a	3.39 (0.4)^{ab}	2.49 (0.5)^b
Chlorophyll (mmol m^{-2})	0.852 (0.14)^a	0.656 (0.064)^a	0.525 (0.074)^a
Chlorophyll *a/b* (mol mol^{-1})	2.92 (0.19)^a	2.78 (0.16)^a	2.33 (0.27)^a
Rubisco/chlorophyll (mmol mol^{-1})	24.6 (1.2)^a	19.9 (1.7)^a	19.8 (1.1)^a
Specific leaf area (m^2 kg^{-1})	3.24 (0.42)^a	1.60 (0.11)^b	1.24 (0.11)^b

Chlorophyll content, Rubisco content and total soluble protein were determined on the same extract used for measurements of k_{catCO2}. Specific leaf area was determined on leaf punches after 5 d of oven drying. Values are means of 5–9 replicates (±SE). Significant differences as determined by ANOVA with P<0.05 are indicated by different letters.

Table 2. Rubisco biochemical parameters at 25 °C, and the corresponding activation energy of the temperature response, from plants grown at three air temperatures.

	Growth temperature		
Parameter	**10 °C**	**20 °C**	**30 °C**
k_{catCO2} (s^{-1})	3.31 (0.09)^a	3.11 (0.08)^b	2.78 (0.10)^c
E_a (kJ mol^{-1})	54.2 (0.83)^a	52.7 (11.9)^a	48.7 (1.7)^a
$S_{C/O}$ (M M^{-1})	75.1 (1.0)^a	76.9 (1.0)^{ab}	78.0 (0.83)^b
E_a (kJ mol^{-1})	−23.7 (1.0)^a	−22.3 (0.37)^{ab}	−19.9 (0.48)^b
K_C(μM)	11.8 (0.49)^a	11.5 (0.52)^a	11.4 (0.70)^a
E_a (kJ mol^{-1})	54.8 (4.4)^a	55.9 (5.6)^a	40.4 (3.3)^b
K_O (μM)	275.6 (7.5)^a	276.1 (13.3)^a	259.7 (35.7)^a
E_a (kJ mol^{-1})	5.47 (0.94)^a	8.81 (4.56)^a	5.94 (1.94)^a

Data represent the mean and SE of 5–7 replicates. Significant differences, as determined by ANOVA (P<0.05), are indicated by different letters.

in temperature response, at 35 °C cold-grown Rubisco K_C was 26% greater than warm-grown Rubisco (Fig. 3C). The Michaelis–Menten constant for O_2 (K_O) did not vary with growth temperature (Table 2; Fig. 3D) and all measurements fell within the 95% confidence intervals of 20 °C-grown Rubisco (Fig. 3D).

Effects of growth temperature on leaf characteristics

There was no significant difference between the amount of chlorophyll or the ratio of chlorophyll *a/b* between plants grown at different temperatures (Table 1). The ratio of Rubisco/chlorophyll appeared 24% larger in cold-grown plants

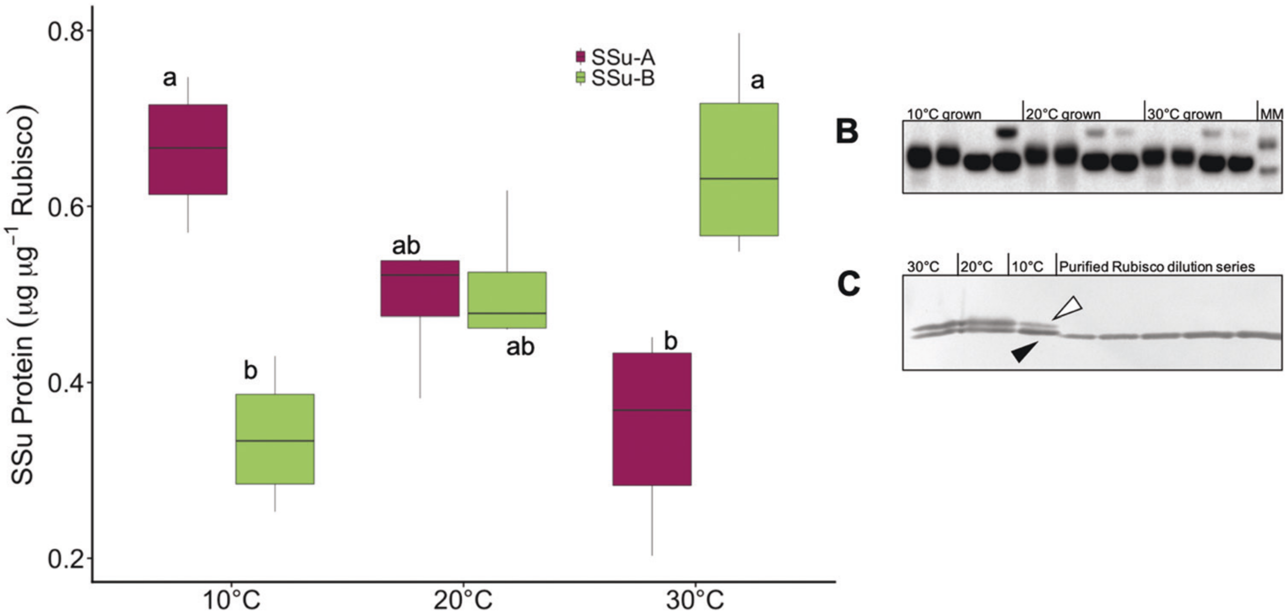

Fig. 2. Rubisco protein expression responses to growth temperature. Rubisco SSu isoform expression (A) based on total soluble protein extracted from Arabidopsis leaves and detected by immunoblotting with an anti-LSu (B) or anti SSu (C) antibody. The first two lanes of each temperature treatment in (B) were extracted with a DTT-free extraction buffer, while the second and third lanes contained 5 mM DTT. In samples extracted with 5 mM DTT, trace amounts (~5%) of LSu peptides migrate in a larger molecular mass complex, consistent with an LSu–SSu cross-linked product. MM, molecular mass ladder. White arrowheads in (C) indicate the SSu-B family proteins, while black arrowheads indicate the SSu-1A protein. The purified Rubisco dilution series from left to right is 0.25, 0.5, 0.9, 1.8, and 2 μg. Each lane in the gel represents one extraction from an individual plant. Rubisco SSu protein expression (A) is reported as the fraction of Rubisco SSu present in either band 1 (SSu-1A, grey) or band 2 (SSu-B family, white) on immunoblots (n=6). Maximum and minimum values are depicted by the bars, the box signifies the upper and lower quartiles, and the median is represented by a short black line within each box. Different letters represent significant differences in the mean of each treatment at P<0.05 (one way ANOVA and post-hoc Tukey's HSD test).

than warm-grown plants (P=0.07; Table 1), but this difference was due to the increased production of Rubisco in cold-grown plants, and not a decrease in chlorophyll content. Warm-grown plants also produced less soluble protein than cold-grown plants (2.5 versus 4.9 mg cm^{-2}), and had 56% lower specific leaf area (Table 1).

Growth temperature impacts on plant gas-exchange: rates, parameters, and limitations

Despite the reduction in Rubisco content in warm-grown plants compared with cold-grown plants (Table 1), estimates of V_{cmax} varied with measurement temperature (P<0.001), but not growth temperature (P=0.22). Estimates of the maximal rate of electron transport (J_{max}) varied with both growth (P=0.0004) and measurement temperature (P=0.0005) such that warm-grown plants had a lower J_{max} at both growth temperatures (Table 3).

Estimated from the initial slope of the A_N–C_c curve *in vivo*, the Rubisco Michaelis–Menten constant under 21% oxygen ($K_{C21\%O2}$) increased with measurement temperature (Table 3), but did not differ with growth temperature when measured at 10 °C. By contrast, cold-grown Arabidopsis plants had a 37% higher $K_{C21\%O2}$ than warm-grown plants when measured at 30 °C (P<0.05; Table 3). Consistent with these observations, the initial slope of the photosynthetic CO_2 response curve was lower in warm- than cold-grown plants measured at 10 °C, but not at 30 °C where warm-grown plants could maintain the same initial slope as cold-grown plants (Fig. 4B). Warm-grown plants had lower photosynthetic rates than cold-grown plants at both measurement temperatures, but the effect was less pronounced at 30 °C. When measured at ambient CO_2 (corresponding to C_a=400 μmol mol^{-1} CO_2, or C_c~170–250 μmol mol^{-1} CO_2), net CO_2 assimilation (A_N) in cold-grown plants was 62% greater than in warm-grown plants at 10 °C, but did not differ from the warm-grown rate of net assimilation at 30 °C (Fig. 4; Table 1). At 30 °C, warm-grown plants maintained higher rates of assimilation on a Rubisco basis, while at 10 °C assimilation rates per Rubisco did not differ between warm- and cold-grown plants (Fig. 4C, D).

Discussion

In this study, we investigated the impact of differential expression of Rubisco small subunit isoforms on carbon assimilation in Arabidopsis. Although previous reports have demonstrated that gene specific expression of the *RbcS* family varies with

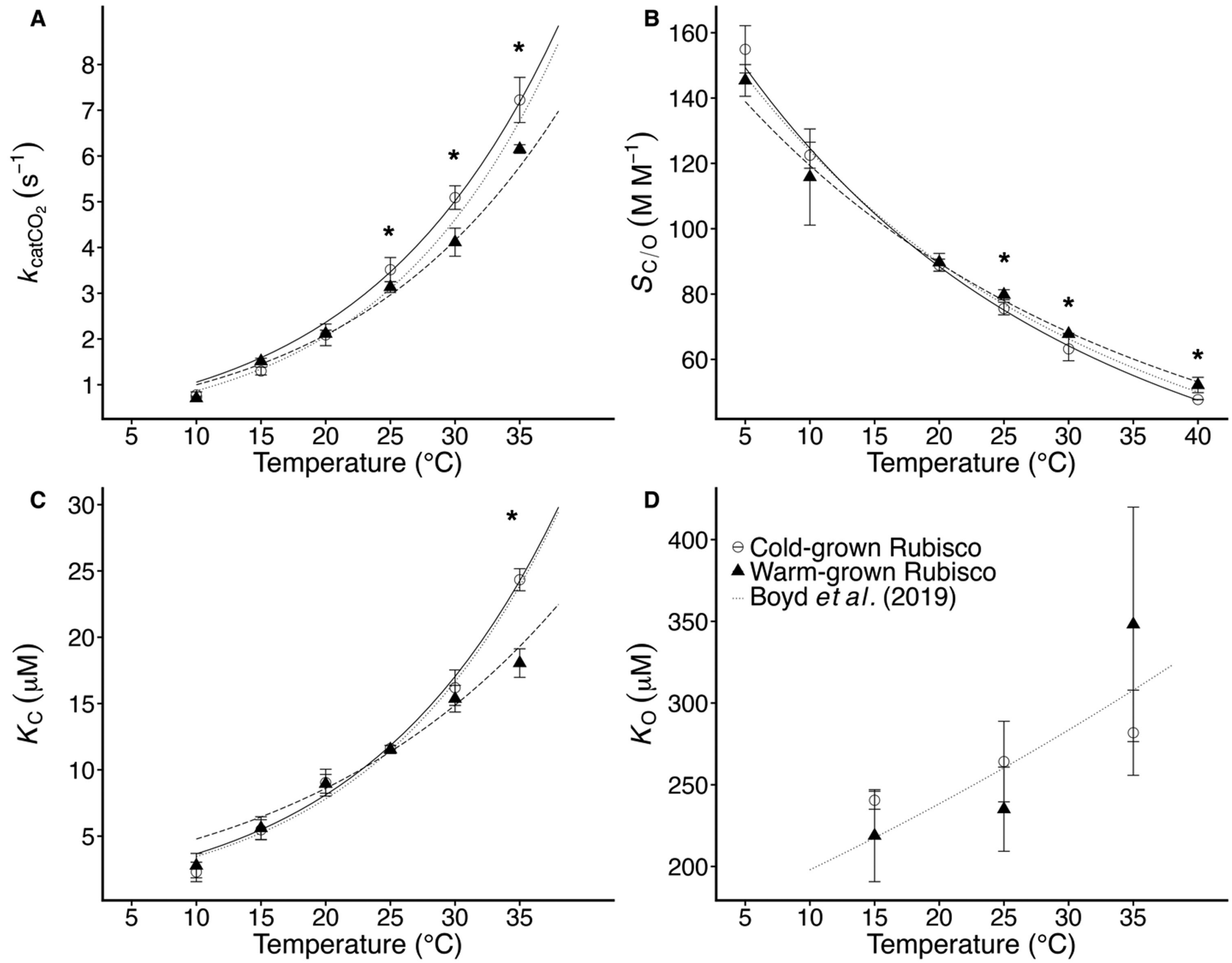

Fig. 3. Temperature response of Rubisco kinetics from cold- and warm-grown Arabidopsis. Temperature dependence of the *in vitro* Rubisco k_{catCO2} (A), $S_{C/O}$ (B), K_C (C), and K_O (D) from warm-grown (triangles) and cold-grown (open circles) Arabidopsis. Parameters were determined by assaying activated Rubisco extracts at the indicated temperatures. Data represent means ±SE of 4–7 replicates. The data for k_{catCO2}, K_C, and $S_{C/O}$ were fitted to: (Parameter(T)=Parameter(25 °C)exp[(T–25)E_a/(298R(273+T))], where R is the universal gas constant (8.314 J K^{-1} mol^{-1}), and T is the temperature in °C. Lines represent the temperature response of cold (solid) and warm (dashed) Rubiscos, and the dotted line is the temperature response from 20 °C-grown Arabidopsis Rubisco as reported in Boyd *et al.*, 2019.

growth condition, impacts on Rubisco catalytic performance or carbon assimilation remain unclear. Here, we demonstrate that in Arabidopsis Rubisco small subunit gene expression and protein production change with growth temperature such that warm-grown plants produce Rubisco containing ~65% SSu-B and cold-grown plants produce Rubisco with ~65% SSu-A as a proportion of the total pool of subunits (Figs 1, 2). These structural changes are accompanied by modifications to Rubisco's performance *in vitro*; warm-grown plants produce a Rubisco having greater CO_2 affinity (i.e. higher $S_{C/O}$ and lower K_C) but lower k_{catCO2} at measurement temperatures above 25 °C (Table 2; Fig. 3). Changes in the kinetic phenotype of Rubisco are also evident *in vivo*, with warm-grown Rubisco having a lower $K_{C21\%O2}$ than cold-grown Rubisco at 30 °C (Table 3). At 30 °C, warm-grown plants maintain assimilation rates similar to cold-grown plants at ambient CO_2 concentrations, despite the latter having 60% more Rubisco on a leaf area basis, indicating that the carboxylation capacity of warm-grown Rubisco is enhanced at warmer measurement temperatures, and is able to compensate for the lower Rubisco content in warm-grown plants (Fig. 4; Table 3). These findings provide insight into Rubisco's performance in a variable climate, which will have increasing importance in a rapidly warming world.

Rubisco SSu isoform expression varies with growth temperature in Arabidopsis

Many photosynthetic proteins exist in multigene families, in which the expression of certain genes is up- or down-regulated in response to changes in the growth environment (Simpson

Table 3. Photosynthetic parameters from cold (10 °C) or warm (30 °C)-grown plants.

	Cold-grown Arabidopsis		Warm-grown Arabidopsis	
	10 °C	**30 °C**	**10 °C**	**30 °C**
A_{400} (μmol CO_2 m^{-2} s^{-1})	19.2 (1.4) [a]	13.2 (2.1) [bc]	11.8 (0.51) [b]	14.7 (0.91) [c]
g_s (mol H_2O m^{-2} s^{-1})	0.26 (0.03) [ab]	0.20 (0.02) [b]	0.44 (0.06) [a]	0.37 (0.11) [ab]
$K_{C21\%O2}$ (μM)	17.7 (4.6) [a]	54.9 (8.5) [b]	15.6 (2.2)[a]	31.7 (4.9)[c]
J_{max} (μmol e^- m^{-2} s^{-1})	133.1 (5.5) [a]	190.6 (16.7) [b]	74.1 (8.2) [c]	138.8 (7.7) [a]
V_{cmax} (μmol CO_2 m^{-2} s^{-1})	55.8 (1.8) [a]	108.1 (7.2) [b]	40.1 (5.0) [a]	100.9 (10.6) [b]
R_d (μmol CO_2 m^{-2} s^{-1})	1.1 (1.4)[a]	3.6 (0.6)[b]	1.1 (0.2)[a]	2.6 (0.3)[c]
g_m (mol CO_2 m^{-2} s^{-1})	0.114 (0.01)[a]	0.142 (0.03)[a]	0.131 (0.03)[a]	0.204 (0.07)[a]

The maximum carboxylation rate (V_{cmax}) and electron transport rate (J_{max}) were estimated from CO_2 assimilation curves measured at 10 °C and 30 °C using the temperature responses of cold- and warm-grown Arabidopsis Rubisco Michaelis–Menten constants for CO_2 and O_2 in Table 1, and the *in vivo* $K_{C21\%O2}$ was estimated from fitting A–C_c curves to the Michaelis–Menten form of the Farquhar model for RuBP saturated photosynthesis. R_d was measured in a dark-acclimated leaf during gas-exchange measurements. Mean values (n=4–7) and SE are reported, and significant differences between values are indicated by different letters according to a two-way ANOVA with P<0.05.

et al., 1986; Green *et al.*, 1991). In Arabidopsis, Rubisco gene expression has been reported to respond to changes in light, CO_2, and growth temperature (Dedonder *et al.*, 1993; Cheng *et al.*, 1998; Yoon *et al.*, 2001; Sawchuk *et al.*, 2008). Typically, these responses involve changes to the total amount of *RbcS* mRNA produced, which correlate well with Rubisco production in many species (Moore *et al.*, 1999). Here, we found that in warm-grown plants, the total *RbcS* transcript abundance decreases by 26% compared with cold-grown plants, and this is coupled with a 38% decrease in Rubisco content (Figs 1, 2), supporting the suggestion that the changes in *RbcS* expression facilitate a coarse control over Rubisco enzyme production (Ogawa *et al.*, 2012). However, Rubisco production involves a number of processes, including transcription, translation and/or post-translation (e.g. protein turnover) events, and availability of the SSu (Berry et al., 1985, 1986; Deng and Gruissem, 1987; Shirley and Meagher, 1990; Suzuki and Makino, 2012; Hanson *et al.*, 2021). Recent work demonstrated that the expression of both *rbcL* and *RbcS* did not match the diel pattern of Rubisco protein abundance in wheat, supporting the importance of post-transcriptional regulation in Rubisco production (Perdomo *et al.*, 2021). Supporting this, we found that cold-grown Arabidopsis plants produce more Rubisco than 20 °C-grown plants (Table 1), but the total *RbcS* mRNA does not increase accordingly (Fig. 1). Additionally, we found that Arabidopsis gene specific *RbcS* expression is coordinated with production of the corresponding SSu peptides in the Rubisco holoenzyme (Figs 1, 2). In Arabidopsis, it seems varied *RbcS* expression has a function beyond the control of Rubisco content.

Arabidopsis Rubisco kinetics vary in response to growth temperature

Rubisco temperature responses across lineages have now been widely characterized, revealing natural variation. Despite general trends for increasing k_{catCO2} and decreasing $S_{C/O}$ with increasing temperature, variation in Rubisco temperature responses exist even among closely related species (Galmés et al., 2015, 2016, 2019; Perdomo *et al.*, 2015; Orr *et al.*, 2016; Sharwood *et al.*, 2016). Early data suggested that environmental factors, such as temperature and availability of CO_2 and O_2, may have selected for 'better' versions of plant Rubiscos whose performance was well adapted to local climate. For example, C_3 species from cool habitats have been found to have an enhanced k_{catCO2} with lower activation energy than warm-native C_3 species, while Mediterranean species native to hot and dry conditions have an increased $S_{C/O}$ (Sage, 2002; Galmés *et al.*, 2005). However, in a meta-analysis of 138 species, incorporating recent large-scale screening of Rubisco temperature responses, these comparisons were found to be non-significant, suggesting limited adaptive changes in Rubisco (Galmés *et al.*, 2019). Further, Orr *et al.* (2016) found that Rubisco from warm temperature environments had increased oxygenation rates and affinity for O_2, resulting in a negative correlation between $S_{C/O}$ and warm temperature environments. Although these results may be impacted by a sampling bias for crop species, or variation in temperature ranges and assay method, potential plasticity in Rubisco temperature response could also have an impact on large-scale screening results. Large multi-species screens, such as that by Orr *et al.* (2016) and Hermida-Carrera *et al.* (2016) represent a common garden experiment, whereby the impacts of growth temperature and climate of origin on Rubisco performance cannot be fully separated.

Here we found that cold-grown Arabidopsis produces Rubisco with a higher k_{catCO2} than warm-grown plants at all measurement temperatures (Fig. 3A; Table 2). The activation energy of k_{catCO2} did not vary with growth temperature, which is consistent with the lack of ecological adaptation noted above. Warm- and cool-grown plants have a similar $S_{C/O}$ at 25 °C, but differences in the apparent activation energy result in warm-grown Rubisco being more specific than cold-grown Rubisco at measurement temperatures above 25 °C (Fig. 3B). This is similar to the acclimation response previously observed in spinach Rubisco (Yamori *et al.*, 2006). The observed changes in Arabidopsis $S_{C/O}$ are likely related to changes in K_c between cold- and warm-grown Rubisco; the increased activation energy of this parameter in cold-grown plants results in a K_c that is 26% greater at 35 °C than that of the warm-grown Rubisco (Table 2; Fig. 3C). Similarly, at low measurement temperatures (<10 °C), cold-hardened *Secale cerale* (winter rye) Rubisco K_c is 50% lower than non-hardened (25 °C grown) Rubisco;

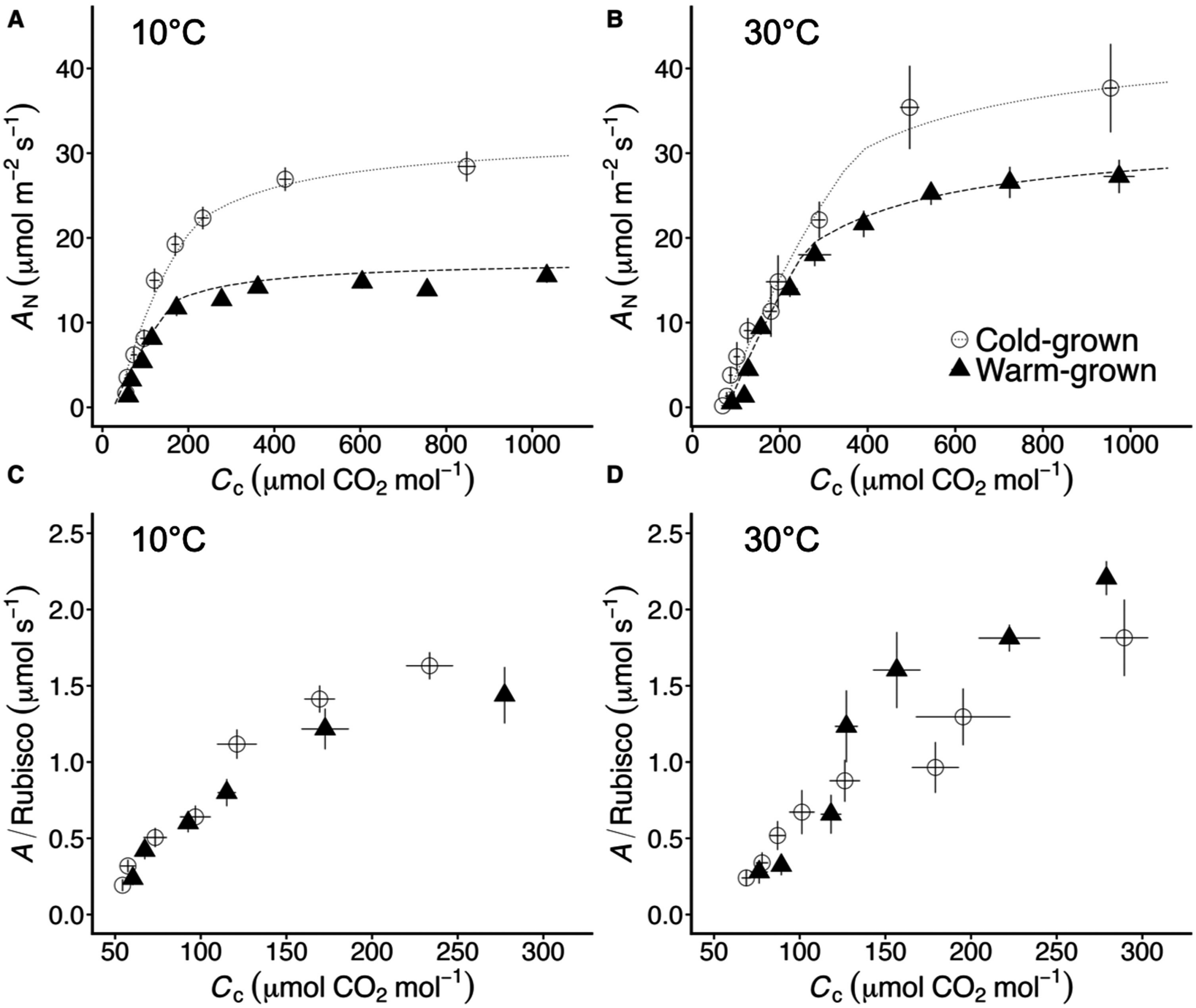

Fig. 4. Photosynthetic carbon assimilation in warm- and cold-grown plants. (A, B) Measured (symbols) and modelled (lines) A–C_c responses of cold-grown (open circles) and warm-grown (triangles) plants at 10 °C (A) and 30 °C (B). The modelled response uses the Rubisco parameters and activation energies reported in Table 2 in the Farquhar *et al.* (1980) model. Other modelling parameters are shown in Table 1. Mesophyll conductance to CO_2 (g_m) was estimated through curve fitting, following Ethier and Livingstone (2004) (see 'Materials and methods'). (C, D) Assimilation per Rubisco concentration at 10 °C (C) and 30 °C (D) as (A_N+R_d)/Rubisco concentration and illustrates changes in Rubisco biochemistry *in vivo* in the Rubisco-limited portion of the A_N–C_c response in (A, B). Data represent means ±SE of 4–7 replicates.

measured above 25 °C, K_c of the cold-hardened enzyme is double that of non-cold-hardened Rubisco (Huner and Macdowall, 1979). It is not clear why low growth temperatures do not confer a biochemical advantage to Rubisco at low measurement temperatures in Arabidopsis, though it may be that increased Rubisco production (Table 1) compensates for any selection pressure for improvement (Fig. 4A, C).

Relationship between SSu isoform abundance and Rubisco performance

Differential expression within multigene families can allow for flexible responses to diverse environmental signals. In barley, the alcohol dehydrogenase (ADH) gene family results in six different ADH isoforms (Hanson and Brown, 1984); the concentration of each isoform responds differently to oxygen levels (Hanson *et al.*, 1984). In maize variable LHCII isoforms accumulate to different levels depending on growth temperature and light conditions; some isoforms increase non-photochemical quenching, suggesting a specific role for variable LHCII complexes (Caffarri *et al.*, 2005). In some species, different isoforms of Rubisco activase are produced at elevated growth temperature, with different rates of ATPase or Rubisco activation, and can impact Rubisco activity and photosynthesis under these conditions (Crafts-Brandner *et al.*, 1997; Law and Crafts-Brandner, 2001; Degen et al., 2020, 2021; Kim *et al.*, 2021). Here, we found that warm-grown Arabidopsis produces more of the SSu-B isoform, and less of SSu-1A, than do cold-grown plants, and the corresponding Rubiscos are more specific for CO_2 versus O_2 at elevated measurement temperatures. This suggests that differential small subunit expression could contribute to plasticity in enzyme function and activity, and may confer on a plant the ability to fine tune Rubisco through the expression of variable SSu isoforms.

We found differences in k_{catCO2} between plants from contrasting growth temperatures at 25 °C, but differences in K_C and $S_{C/O}$ were only apparent at measurement temperatures above 35 °C, highlighting the need to measure Rubisco kinetics under more than one measurement temperature. Previous work has also demonstrated that mutations in Arabidopsis Rubisco SSu isoforms do not impact photosynthesis or holoenzyme kinetic properties under the present atmospheric CO_2 concentrations at measurement temperatures of 25 °C (Izumi *et al.*, 2012; Atkinson *et al.*, 2017). Lin *et al.* (2020) investigated the impact of homogeneous SSu composition in recombinant tobacco Rubisco and found no differences in Rubisco kinetics at 25 °C attributed to subunit composition beyond the increased k_{catCO2} and lower K_C conferred by the distinct trichome SSu (Laterre *et al.*, 2017; Lin *et al.*, 2020). This supports earlier attempts to mix and match tobacco Rubisco subunits via interspecific hybridizations, which also found no impact of SSu composition on Rubisco activity (Li *et al.*, 1983). However, the kinetics of potato Rubisco expressed in tobacco were significantly affected by the identity of the SSu (Martin-Avila *et al.*, 2020), and a recent survey of recombinant Solanaceae ancestral Rubisco suggests that the SSu influences the kinetic phenotype of the enzyme, in particular at warmer temperatures (Lin *et al.*, 2022). The minor differences in the Arabidopsis SSu polypeptides are found in regions known to influence Rubisco kinetics in other organisms (Valegard *et al.*, 2018) and may play a role in holoenzyme stability or CO_2 affinity (van Lun *et al.*, 2014; Poudel *et al.*, 2020), which would have a pronounced impact at elevated temperatures.

Plant acclimation to growth temperature: Rubisco responses in vivo

We demonstrated that growth temperature alters Arabidopsis Rubisco kinetic performance *in vitro* and growth-temperature induced changes in Rubisco biochemistry are also evident *in vivo*, with warm-grown Rubisco having a lower apparent $K_{C21\%O2}$ than cold-grown Rubisco at 30 °C (Table 3). Additionally, there is no difference in the initial slope of the photosynthetic CO_2 response between warm- and cold-grown plants at 30 °C, indicating that the enhanced carboxylation capacity of warm-grown Rubisco compensates for the lower Rubisco content in warm-grown plants (Fig. 4A, B; Table 3). As a result, warm-grown plants maintain rates of CO_2 assimilation (*A*) similar to cold-grown plants at 30 °C and ambient (or lower) CO_2 concentrations, despite their reduced Rubisco content (Fig. 4C, D). This ability could provide a photosynthetic advantage during times of stomatal closure, such as drought conditions, which are frequently associated with growth at elevated temperatures in natural and agricultural systems.

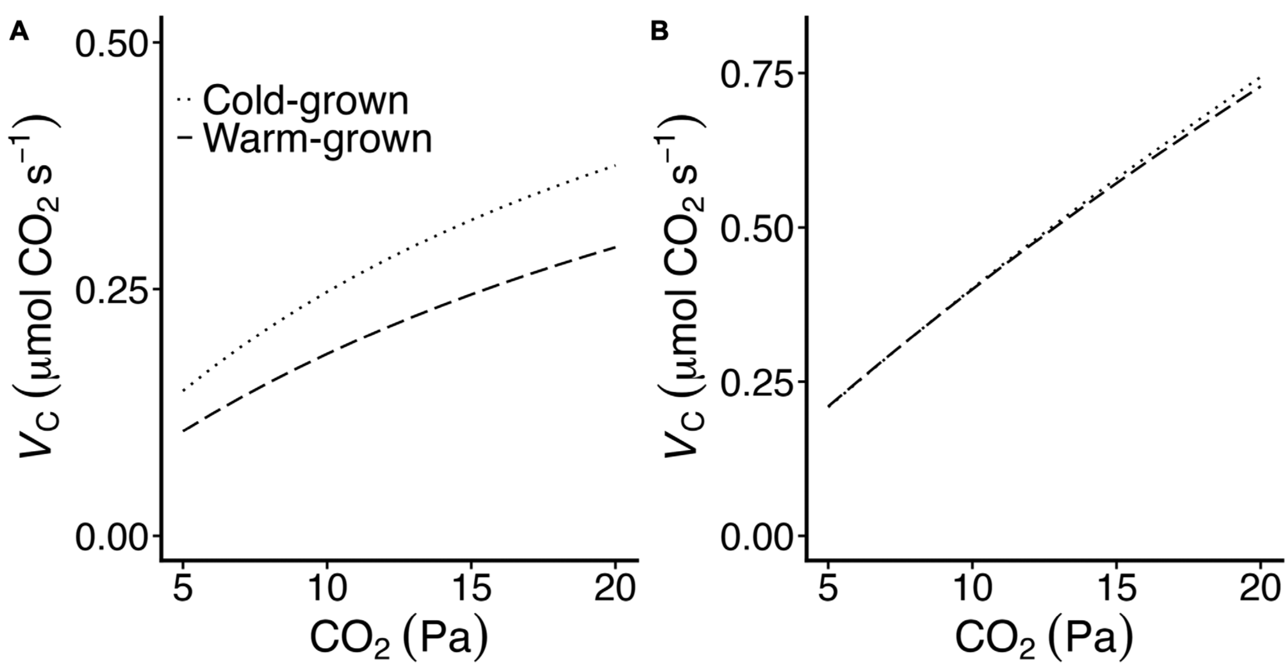

Fig. 5. Modelled responses of Rubisco carboxylation accounting for differences in growth temperature changes to kinetics. The impact of changes in Rubisco K_C (Table 2) are modelled for cold-grown (dotted line) and warm-grown (dashed line) Rubisco at 10 °C (A) and 30 °C (B).

In spinach, similar changes in Rubisco performance offer a theoretical carbon assimilation advantage to a warm-grown plant (Cavanagh and Kubien, 2014). However, when changes in spinach Rubisco $S_{C/O}$ are driven by differences in K_C, as they appear to be in Arabidopsis (Table 2; Fig. 3), a carbon gain advantage for a warm-grown plant is only found at temperatures greater than approximately 32–33 °C (i.e. at temperatures above the growth temperature). When the observed differences in K_C are used to model the rate of Rubisco carboxylation on an equal enzyme concentration basis (i.e. V_C), the initial slopes of the CO_2 response are similar at 30 °C, but not 10 °C (Fig. 5), similar to the results of our *in vivo* CO_2 response curve. However, at ambient and higher CO_2 concentrations, the lower photosynthetic rate in warm-grown plants is a likely result of strict limitations imposed by decreased Rubisco content; warm-grown plants produce 38% less Rubisco than cold-grown plants (Table 1). Warm-grown plants do maintain rates of CO_2 assimilation similar to cold-grown plants at 30 °C and at ambient and sub-ambient CO_2 concentration (Fig. 4B), which is likely a reflection of their lower $K_{C21\%O2}$ and higher $S_{C/O}$ at this temperature.

Effects of Rubisco phenotypic plasticity on photosynthetic performance and modelling

Plasticity in Rubisco performance may have important implications for modelling photosynthesis, as the CO_2 assimilation rate of most species is modelled using *in vivo* Rubisco kinetic parameters obtained from tobacco or Arabidopsis, and the effect of growth environment on Rubisco performance or content is not considered (Bernacchi *et al.*, 2001; Walker *et al.*, 2013). Further, *in vivo* Rubisco temperature responses in Arabidopsis and tobacco have been obtained using an antisense knockdown of a single *RbcS* gene, which may bias the temperature response. Despite the lack of species-specific differences in a single Rubisco biochemical parameter between Arabidopsis and tobacco grown at the same temperature, estimates of V_{cmax} obtained from a CO_2 response curve vary depending on the choice of temperature response parameters used, highlighting the importance of small variation in Rubisco parameters for modelling photosynthesis (Walker *et al.*, 2013). The effect of growth temperature-induced changes, or modulations via the SSu, particularly on $S_{C/O}$, K_C, and their activation energies (Table 2), could result in species-specific differences between parameters that impact photosynthetic models.

Supplementary data

The following supplementary data are available at *JXB* online.

Fig. S1. Combinatorial temperature and CO_2 treatments on *RbcS* expression.

Fig. S2. Response of low abundance *RbcS* isoforms to growth temperature.

Fig. S3. Temperature response of Rubisco $S_{C/O}$ above 20 °C.

Table S1. A list of primers used in this work.

Author contributions

APC and DSK designed the original research questions. APC performed the experiments, and collected the data. APC analysed the data with support from all co-authors. APC led the writing of the manuscript with contributions from all authors.

Conflict of interest

The authors have no conflicts to declare.

Funding

This work was supported by a National Science and Engineering Research Council of Canada (NSERC) Discovery grant (327103-2008) to DSK. APC was supported by an NSERC PGS-D scholarship and fellowship from the O'Brien Foundation.

Data availability

The data are available upon request from the corresponding author (APC).

References

Andrews TJ. 1988. Catalysis by cyanobacterial ribulose-bisphosphate carboxylase large subunits in the complete absence of small subunits. Journal of Biological Chemistry **263**, 12213–12219.

Atkinson N, Leitão N, Orr DJ, Meyer MT, Carmo-Silva E, Griffiths H, Smith AM, McCormick AJ. 2017. Rubisco small subunits from the unicellular green alga *Chlamydomonas* complement Rubisco-deficient mutants of Arabidopsis. New Phytologist **214**, 655–667.

Bernacchi CJ, Singsaas EL, Pimentel C, Portis AR Jr, Long SP. 2001. Improved temperature response functions for models of Rubisco-limited photosynthesis. Plant, Cell & Environment **24**, 253–259.

Berry JO, Nikolau BJ, Carr JP, Klessig DF. 1985. Transcriptional and post-transcriptional regulation of ribulose 1,5-bisphosphate carboxylase gene expression in light- and dark-grown amaranth cotyledons. Molecular and Cellular Biology **5**, 2238–2246.

Berry JO, Nikolau BJ, Carr JP, Klessig DF. 1986. Translational regulation of light-induced ribulose 1,5-bisphosphate carboxylase gene expression in amaranth. Molecular and Cellular Biology **6**, 2347–2353.

Boyd RA, Cavanagh AP, Kubien DS, Cousins AB. 2019. Temperature response of Rubisco kinetics in *Arabidopsis thaliana*: thermal breakpoints and implications for reaction mechanisms. Journal of Experimental Botany **70**, 231–242.

Bradford MM. 1976. A rapid and sensitive method for the quantitation of microgram quantities of protein utilizing the principle of protein-dye binding. Analytical Biochemistry **72**, 248–254.

Caffarri S, Frigerio S, Olivieri E, Righetti PG, Bassi R. 2005. Differential accumulation of *Lhcb* gene products in thylakoid membranes of *Zea* *mays* plants grown under contrasting light and temperature conditions. Proteomics **5**, 758–768.

Cavanagh AP. 2020. Big progress for small subunits: new Rubisco mutants in Arabidopsis. Journal of Experimental Botany **71**, 5721–5724.

Cavanagh AP, Kubien DS. 2014. Can phenotypic plasticity in Rubisco performance contribute to photosynthetic acclimation? Photosynthesis Research **119**, 203–214.

Cavanagh AP, South PF, Bernacchi CJ, Ort DR. 2022. Alternative pathway to photorespiration protects growth and productivity at elevated temperatures in a model crop. Plant Biotechnology Journal **20**, 711–721.

Cheng S-H, Moore B, Seemann JR. 1998. Effects of short- and long-term elevated CO_2 on the expression of ribulose-1,5-bisphosphate carboxylase/oxygenase genes and carbohydrate accumulation in leaves of *Arabidopsis thaliana* (L.) Heynh. Plant Physiology **116**, 715–723.

Crafts-Brandner SJ, van de Loo FJ, Salvucci ME. 1997. The two forms of ribulose-1,5-bisphosphate carboxylase/oxygenase activase differ in sensitivity to elevated temperature. Plant Physiology **114**, 439–444.

Czechowski T, Stitt M, Altmann T, Udvardi MK, Scheible W-R. 2005. Genome-wide identification and testing of superior reference genes for transcript normalization in Arabidopsis. Plant Physiology **139**, 5–17.

Dedonder A, Roger R, Fredericq H, Van Montagu M, Krebbers E. 1993. Arabidopsis *RbcS* genes are differentially regulated by light. Plant Physiology **101**, 801–808.

Degen GE, Orr DJ, Carmo-Silva E. 2021. Heat-induced changes in the abundance of wheat Rubisco activase isoforms. New Phytologist **229**, 1298–1311.

Degen GE, Worrall D, Carmo-Silva E. 2020. An isoleucine residue acts as a thermal and regulatory switch in wheat Rubisco activase. The Plant Journal **103**, 742–751.

Deng XW, Gruissem W. 1987. Control of plastid gene expression during development: the limited role of transcriptional regulation. Cell **49**, 379–387.

Eilenberg H, Hanania U, Stein H, Zilberstein A. 1998. Characterization of *RbcS* genes in the fern *Pteris vittata* and their photoregulation. Planta **206**, 204–214.

Ethier GJ, Livingston NJ. 2004. On the need to incorporate sensitivity to CO_2 transfer conductance into the Farquhar–von Caemmerer–Berry leaf photosynthesis model. Plant, Cell & Environment **27**, 137–153.

Ethier GJ, Livingston NJ, Harrison DL, Black TA, Moran JA. 2006. Low stomatal and internal conductance to CO_2 versus Rubisco deactivation as determinants of the photosynthetic decline of ageing evergreen leaves. Plant, Cell & Environment **29**, 2168–2184.

Farquhar GD, von Caemmerer S, Berry JA. 1980. A biochemical model of photosynthetic CO_2 assimilation in leaves of C_3 species. Planta **149**, 78–90.

Flexas J, Ortuño MF, Ribas-Carbo M, Diaz-Espejo A, Flórez-Sarasa ID, Medrano H. 2007. Mesophyll conductance to CO_2 in *Arabidopsis thaliana*. New Phytologist **175**, 501–511.

Galmés J, Capó-Bauçà S, Niinemets U, Iñiguez C. 2019. Potential improvement of photosynthetic CO_2 assimilation in crops by exploiting the natural variation in the temperature response of Rubisco catalytic traits. Current Opinion in Plant Biology **49**, 60–67.

Galmés J, Flexas J, Keys AJ, Cifre J, Mitchell RAC, Madgwick PJ, Haslam RP, Medrano H, Parry MAJ. 2005. Rubisco specificity factor tends to be larger in plant species from drier habitats and in species with persistent leaves. Plant, Cell & Environment **28**, 571–579.

Galmés J, Hermida-Carrera C, Laanisto L, Niinemets Ü. 2016. A compendium of temperature responses of Rubisco kinetic traits: variability among and within photosynthetic groups and impacts on photosynthesis modeling. Journal of Experimental Botany **67**, 5067–5091.

Galmés J, Kapralov MV, Copolovici LO, Hermida-Carrera C, Niinemets Ü. 2015. Temperature responses of the Rubisco maximum carboxylase activity across domains of life: phylogenetic signals, trade-offs, and importance for carbon gain. Photosynthesis Research **123**, 183–201.

Getzoff TP, Zhu G, Bohnert HJ, Jensen RG. 1998. Chimeric *Arabidopsis thaliana* ribulose-1,5-bisphosphate carboxylase/oxygenase containing a pea small subunit protein is compromised in carbamylation. Plant Physiology **116**, 695–702.

Green BR, Pichersky E, Kloppstech K. 1991. Chlorophyll *a*/*b*-binding proteins: an extended family. Trends in Biochemical Sciences **16**, 181–186.

Hanson AD, Brown AHD. 1984. Three alcohol dehydrogenase genes in wild and cultivated barley: Characterization of the products of variant alleles. Biochemical Genetics **22**, 495–515.

Hanson AD, Jacobsen JV, Zwar JA. 1984. Regulated expression of three alcohol dehydrogenase genes in barley aleurone layers. Plant Physiology **75**, 573–581.

Hanson AD, McCarty DR, Henry CS, Xian X, Joshi J, Patterson JA, García-García JD, Fleischmann SD, Tivendale ND, Millar AH. 2021. The number of catalytic cycles in an enzyme's lifetime and why it matters to metabolic engineering. Proceedings of the National Academy of Sciences, USA **118**, e2023348118.

Hermida-Carrera C, Kapralov MV, Galmés J. 2016. Rubisco catalytic properties and temperature response in crops. Plant Physiology **171**, 2549–2561.

Huner NP, Macdowall FD. 1979. The effects of low temperature acclimation of winter rye on catalytic properties of its ribulose bisphosphate carboxylase-oxygenase. Canadian Journal of Biochemistry **57**, 1036–1041.

Ishikawa C, Hatanaka T, Misoo S, Miyake C, Fukayama H. 2011. Functional incorporation of sorghum small subunit increases the catalytic turnover rate of Rubisco in transgenic rice. Plant Physiology **156**, 1603–1611.

Izumi M, Tsunoda H, Suzuki Y, Makino A, Ishida H. 2012. *RBCS1A* and *RBCS3B*, two major members within the *Arabidopsis RBCS* multigene family, function to yield sufficient Rubisco content for leaf photosynthetic capacity. Journal of Experimental Botany **63**, 2159–2170.

Kapralov MV, Kubien DS, Andersson I, Filatov DA. 2010. Changes in Rubisco kinetics during the evolution of C_4 photosynthesis in *Flaveria* (Asteraceae) are associated with positive selection on genes encoding the enzyme. Molecular Biology and Evolution **28**, 1491–1503.

Khumsupan P, Kozlowska MA, Orr DJ, Andreou AI, Nakayama N, Patron N, Carmo-Silva E, McCormick AJ. 2020. Generating and characterizing single- and multigene mutants of the Rubisco small subunit family in Arabidopsis. Journal of Experimental Botany **71**, 5963–5975.

Kim SY, Slattery RA, Ort DR. 2021. A role for differential Rubisco activase isoform expression in C_4 bioenergy grasses at high temperature. GCB Bioenergy **13**, 211–223.

Kubien DS, Brown CM, Kane HJ. 2011. Quantifying the amount and activity of Rubisco in leaves. Methods in Molecular Biology **684**, 349–362.

Laterre R, Pottier M, Remacle C, Boutry M. 2017. Photosynthetic trichomes contain a specific Rubisco with a modified pH-dependent activity. Plant Physiology **173**, 2110–2120.

Law RD, Crafts-Brandner SJ. 2001. High temperature stress increases the expression of wheat leaf ribulose-1,5-bisphosphate carboxylase/oxygenase activase protein. Archives of Biochemistry and Biophysics **386**, 261–267.

Li LR, Verne AS, Kung SD. 1983. Relationship between the kinetic properties and the small subunit composition of *Nicotiana* ribulose-1, 5-bisphosphate carboxylase. Plant Physiology **71**, 404–408.

Lin MT, Salihovic H, Clark FK, Hanson MR. 2022. Improving the efficiency of Rubisco by resurrecting its ancestors in the family Solanaceae. Science Advances **8**, eabm6871.

Lin MT, Stone WD, Chaudhari V, Hanson MR. 2020. Small subunits can determine enzyme kinetics of tobacco Rubisco expressed in *Escherichia coli*. Nature Plants **6**, 1289–1299.

Lundgren MR, Christin P-A. 2016. Despite phylogenetic effects, C_3–C_4 lineages bridge the ecological gap to C_4 photosynthesis. Journal of Experimental Botany **68**, 241–254.

Martin-Avila E, Lim Y-L, Birch R, Dirk LMA, Buck S, Rhodes T, Sharwood RE, Kapralov MV, Whitney SM. 2020. Modifying plant photosynthesis and growth via simultaneous chloroplast transformation of rubisco large and small subunits. The Plant Cell **32**, 2898–2916.

Meier I, Kristie LC, Fleming AJ, Gruissem W. 1995. Organ-specific differential regulation of a promoter subfamily for the ribulose-1,5-bisphosphate carboxylase/oxygenase small subunit genes in tomato. Plant Physiology **107**, 1105–1118.

Moore BD, Cheng S-H, Sims D, Seemann JR. 1999. The biochemical and molecular basis for photosynthetic acclimation to elevated atmospheric CO_2. Plant, Cell & Environment **22**, 567–582.

Moore CE, Meacham-Hensold K, Lemonnier P, Slattery RA, Benjamin C, Bernacchi CJ, Lawson T, Cavanagh AP. 2021. The effect of increasing temperature on crop photosynthesis: from enzymes to ecosystems. Journal of Experimental Botany **72**, 2822–2844.

Ogawa S, Suzuki Y, Yoshizawa R, Kanno K, Makino A. 2012. Effect of individual suppression of *RBCS* multigene family on Rubisco contents in rice leaves. Plant, Cell & Environment **35**, 546–553.

Orr DJ, Alcântara A, Kapralov MV, Andralojc PJ, Carmo-Silva E, Parry MAJ. 2016. Surveying Rubisco diversity and temperature response to improve crop photosynthetic efficiency. Plant Physiology **172**, 707–717.

Perdomo JA, Buchner P, Carmo-Silva E. 2021. The relative abundance of wheat Rubisco activase isoforms is post-transcriptionally regulated. Photosynthesis Research **148**, 47–56.

Perdomo JA, Cavanagh AP, Kubien DS, Galmés J. 2015. Temperature dependence of in vitro Rubisco kinetics in species of *Flaveria* with different photosynthetic mechanisms. Photosynthesis Research **124**, 67–75.

Porra RJ, Thompson WA, Kriedemann PE. 1989. Determination of accurate extinction coefficients and simultaneous equations for assaying chlorophylls *a* and *b* extracted with four different solvents: verification of the concentration of chlorophyll standards by atomic absorption spectroscopy. Biochimica et Biophysica Acta – Bioenergetics **975**, 384–394.

Poudel S, Pike DH, Raanan H, Mancini JA, Nanda V, Rickaby RE, Falkowski PG. 2020. Biophysical analysis of the structural evolution of substrate specificity in RuBisCO. Proceedings of the National Academy of Sciences, USA **117**, 30451–30457.

R Core Team. 2020. R: A language and environment for statistical computing. Vienna: R Foundation for Statistical Computing.

Roell M-S, Borzyskowski LS, Westhoff P, Plett A, Paczia N, Claus P, Schlueter U, Erb TJ, Weber APM. 2021. A synthetic C4 shuttle via the β-hydroxyaspartate cycle in C3 plants. Proceedings of the National Academy of Sciences, USA **118**, e2022307118.

Sage RF. 2002. Variation in the k_{cat} of Rubisco in C_3 and C_4 plants and some implications for photosynthetic performance at high and low temperature. Journal of Experimental Botany **53**, 609–620.

Sage RF, Kubien DS. 2007. The temperature response of C_3 and C_4 photosynthesis. Plant, Cell & Environment **30**, 1086–1106.

Sage RF, Monson RK, Ehleringer JR, Adachi S, Pearcy RW. 2018. Some like it hot: the physiological ecology of C_4 plant evolution. Oecologia **187**, 941–966.

Sawchuk MG, Donner TJ, Head P, Scarpella E. 2008. Unique and overlapping expression patterns among members of photosynthesis-associated nuclear gene families in Arabidopsis. Plant Physiology **148**, 1908–1924.

Sharwood RE, Ghannoum O, Kapralov MV, Gunn LH, Whitney SM. 2016. Temperature responses of Rubisco from Paniceae grasses provide opportunities for improving C_3 photosynthesis. Nature Plants **2**, 16186.

Shirley BW, Meagher RB. 1990. A potential role for RNA turnover in the light regulation of plant gene expression: ribulose-1,5-bisphosphate carboxylase small subunit in soybean. Nucleic Acids Research **18**, 3377–3385.

Simpson J, Van Montagu M, Herrera-Estrella L. 1986. Photosynthesis-associated gene families: differences in response to tissue-specific and environmental factors. Science **233**, 34–38.

South PF, Cavanagh AP, Liu HW, Ort DR. 2019. Synthetic glycolate metabolism pathways stimulate crop growth and productivity in the field. Science **363**, eaat9077.

Spreitzer RJ. 2003. Role of the small subunit in ribulose-1,5-bisphosphate carboxylase/oxygenase. Archives of Biochemistry and Biophysics **414**, 141–149.

Spreitzer RJ, Peddi SR, Satagopan S. 2005. Phylogenetic engineering at an interface between large and small subunits imparts land-plant kinetic properties to algal Rubisco. Proceedings of the National Academy of Sciences, USA **102**, 17225–17230.

Suzuki Y, Makino A. 2012. Availability of Rubisco small subunit up-regulates the transcript levels of large subunit for stoichiometric assembly of its holoenzyme in rice. Plant Physiology **160**, 533–540.

Suzuki Y, Miyamoto T, Yoshizawa R, Mae T, Makino A. 2009. Rubisco content and photosynthesis of leaves at different positions in transgenic rice with an overexpression of *RBCS*. Plant, Cell & Environment **32**, 417–427.

Valegard K, Hasse D, Andersson I, Gunn LH. 2018. Structure of Rubisco from *Arabidopsis thaliana* in complex with 2-carboxyarabinitol-1,5-bisphosphate. Acta Crystallographica Section D **74**, 1–9.

van Lun M, Hub JS, van der Spoel D, Andersson I. 2014. CO_2 and O_2 distribution in Rubisco suggests the small subunit functions as a CO_2 reservoir. Journal of the American Chemical Society **136**, 3165–3171.

Walker B, Ariza LS, Kaines S, Badger MR, Cousins AB. 2013. Temperature response of *in vivo* Rubisco kinetics and mesophyll conductance in *Arabidopsis thaliana*: comparisons to *Nicotiana tabacum*. Plant, Cell & Environment **36**, 2108–2119.

Walker BJ, VanLoocke A, Bernacchi CJ, Ort DR. 2016. The costs of photorespiration to food production now and in the future. Annual Review of Plant Biology **67**, 107–129.

Wanner LA, Gruissem W. 1991. Expression dynamics of the tomato *RbcS* gene family during development. The Plant Cell **3**, 1289–1303.

Yamori W, Suzuki K, Noguchi K, Nakai M, Terashima I. 2006. Effects of Rubisco kinetics and Rubisco activation state on the temperature dependence of the photosynthetic rate in spinach leaves from contrasting growth temperatures. Plant, Cell & Environment **29**, 1659–1670.

Yamori W, von Caemmerer S. 2011. Quantification of Rubisco activase content in leaf extracts. Methods in Molecular Biology **684**, 383–391.

Yoon M, Putterill JJ, Ross GS, Laing WA. 2001. Determination of the relative expression levels of rubisco small subunit genes in Arabidopsis by rapid amplification of cDNA ends. Analytical Biochemistry **291**, 237–244.